Measurement-based Optimal DER Dispatch with a Recursively Estimated Sensitivity Model

Severin Nowak, *Student Member, IEEE,* Yu Christine Chen, *Member, IEEE,* and Liwei Wang, *Member, IEEE*

***Abstract*—This paper presents a measurement-based method to determine distributed energy resource (DER) active- and reactive-power setpoints that minimize bus voltage deviations from prescribed reference values, bus active- and reactive-power deviations from desired setpoints, as well as cost of DER outputs. Central to the proposed method is the estimation of a linear sensitivity model from synchronized voltage and power-injection data collected from distribution-level phasor measurement units installed at only a subset of buses in the distribution system. As new measurements become available, the linear sensitivity model is updated via the recursive weighted partial least-squares estimation method. The estimated sensitivity model is then embedded as an equality constraint in a convex quadratic optimization problem, which can be solved via, e.g., the alternating direction method of multipliers. Numerical simulations involving the IEEE 33-bus distribution test system illustrate key benefits of the proposed method, including (i) eliminating the need for an accurate offline system model, (ii) adapting to online network-topology and operating-point changes, and (iii) being robust against delays potentially attributed to communication, computation, and actuation. Additional numerical simulations involving larger test systems demonstrate computational scalability.**

***Index Terms*—Distributed energy resources, measurement-based method, model estimation, optimal DER dispatch, partial least-squares estimation.**

I. Introduction

INTEGRATION of distributed energy resources (DERs), such as rooftop solar-photovoltaic and battery-storage systems, helps to alleviate environmental concerns of conventional fossil fuel-based generation. Moreover, DERs can help to regulate voltages at the distribution level by providing reactive-power support, and their active-power outputs can be coordinated toward frequency regulation for the transmission system [1], [2]. Reliable and efficient operation of the integrated power grid has motivated recent research into developing DER management systems. These generally involve repeated solutions of optimization problems constrained by the nonlinear network power balance, DER capacity limits, and other operational limits. Such methods may be computationally burdensome in practical field implementation, especially with rapidly varying operating point [3]. Moreover, many require an accurate and up-to-date network model that may not be available in real time, resulting in DER setpoints that lead to unexpected or undesired system behaviour [4].

In this work, we use synchronized bus-voltage and power-injection measurements collected from distribution-level phasor measurement units (D-PMUs) installed at a subset of the buses in the distribution system to estimate a linear sensitivity model that approximates the relationship between voltages and power injections at measured buses. The D-PMUs provide time-synchronized voltage- and current-phasor measurements with phase-angle accuracy of $0.01°$; and they stream the phasor data through a standard communication interface (e.g., IEEE C37.118) at intervals in the sub-second range [4]. These properties are sufficient to ensure that the estimated sensitivity model reflects up-to-date system attributes [5]. We then embed the estimated model in an optimal DER dispatch problem as a linear constraint, replacing the nonlinear power-balance equations. In so doing, the proposed approach is amenable to real-world implementation of DER management systems because, compared to versions of the optimization problem with nonlinear constraints, it incurs lower computational burden to obtain sufficiently accurate optimal DER dispatch solutions. Moreover, the proposed approach does not rely on any prior knowledge about a network model, and the resulting DER dispatch adapts to the system's evolving operating point and network topology.

With the above in mind, we focus our review of relevant literature squarely on measurement-based methods for (i) online model estimation, and (ii) optimal DER dispatch, both in distribution systems. (A review of other applications, such as state estimation, event detection, and phase identification, can be found in [4]). Several lines of research infer the distribution network topology by recovering the admittance matrix with graph theoretical approaches [6], using maximum-likelihood estimation with error-in-variable models [7], actively probing smart inverters to estimate the grid Laplacian [8], developing low-complexity algorithms [9], and leveraging convex-optimization techniques [10]. Prior art has also tackled online estimation of other system attributes, including injection shift factors [11], the power-flow Jacobian [12], linearized power-flow models [5], and power-to-voltage sensitivities [13], [14].

Shifting attention to methods for measurement-based DER dispatch, [15] leverages estimated power-to-voltage sensitivities to determine DER setpoints that regulate the voltage profile across a distribution network. In order to reduce the number of samples needed to estimate the sensitivities, [15] assumes prior knowledge of feasible topology configurations and line resistance-to-reactance ratios. Voltage regulation is also the objective in [16], where rule- and optimization-based control schemes are deployed in conjunction with an estimated second-order power-flow sensitivity model. Furthermore, [17] optimizes DER setpoints to regulate the active-power injection from the distribution feeder into the transmission grid while relying on prior knowledge of network topology. Another line of related work solves the optimal power flow problem

Severin Nowak and Liwei Wang are with the School of Engineering at The University of British Columbia, Okanagan Campus, Kelowna, Canada. E-mail: {severin.nowak, liwei.wang}@ubc.ca. Yu Christine Chen is with the Department of Electrical and Computer Engineering at The University of British Columbia, Vancouver, Canada. E-mail: chen@ece.ubc.ca. This work was supported by Mitacs through the Mitacs Accelerate program with industrial partner Enbala Power Networks Inc.

via quasi-Newton methods aided by real-time measurements of values and constraints of decision variables [18]. Also, feedback optimization is used to synthesize controllers to achieve distribution-level voltage regulation in centralized fashion [19], [20] and distributed manner [21]–[23]. Combined control of system voltages and substation power setpoints is accomplished via primal-dual gradient methods to solve a saddle-point problem in a distributed fashion in [3], and the framework is extended to include aggregations of DERs, multi-phase systems, and discrete DER setpoints through a bilevel optimization formulation in [24]. However, the aforementioned feedback optimization methods all rely on some (albeit possibly limited) knowledge of the underlying power network structure to compute relevant gradients and Hessians. Model-free combined voltage and active-power control via an extremum seeking approach is developed in [25], and it is extended to unbalanced systems to regulate line flows in [26].

In this paper, we propose a measurement-based approach, which does not rely on any prior knowledge of or even regard for the underlying network topology, to determine DER active- and reactive-power setpoints aimed at regulating bus voltages and injections as well as minimizing DER costs. The proposed framework consists of two successive and iterative stages: (i) sensitivity model estimation, and (ii) optimal DER dispatch. This paper builds on preliminary work reported in [27] and provides extensions in several directions. For the estimation stage, we remove the requirement of equipping D-PMUs at all buses in the distribution system for estimating the linear voltage-to-power sensitivity model with online measurements of bus voltage phasors and active- and reactive-power injections. We also leverage the recursive weighted partial least-squares (RWPLS) algorithm to improve (i) the practicality of the proposed approach by performing recursive updates, and (ii) its adaptability to network-topology and operating-point changes by placing more weight on recent measurements and less on past ones. The resulting estimated model contains key sensitivity characteristics amongst measured quantities without explicitly recovering the grid topology or power-flow model as in [5]–[10]. It is worth noting that while non-recursive variants of least-squares estimation have been used to compute linearized power-flow models [5], the power-flow Jacobian matrix [12], and power-to-voltage sensitivities [13], to the best of our knowledge, the RWPLS algorithm has not been utilized for applications in the power systems domain.

In the DER dispatch stage, we incorporate the estimated linear sensitivity model into a convex quadratic optimization problem. As a direct consequence, the optimal dispatch is solved without any offline knowledge of the underlying network, distinct from methods in [3], [19]–[24]. Also, unlike [15]–[17], [19]–[23], our proposed formulation achieves combined objectives of minimizing (i) DER active- and reactive-power costs and (ii) deviations of bus voltages and injections from their respective reference values. Moreover, compared with [25], [26], our proposed method uses lower temporal measurement resolution and smaller injection perturbations. Extensive numerical simulations demonstrate that the proposed measurement-based optimal DER dispatch adapts to unexpected operating-point and network-topology changes and closely matches the model-based optimal dispatch solved with accurate system model. Also via numerical simulations, we evaluate the impact of DER dynamics, delays potentially attributed to communication, computation, and actuation, and RWPLS parameters on the performance of the proposed method. Furthermore, we illustrate the flexibility of the proposed framework by accommodating typical constraints on DER active- and reactive-power outputs. Finally, we report execution times involved with the model estimation and optimal dispatch stages of the proposed framework.

The remainder of this paper is organized as follows. In Section II, we describe the network and power-flow model, present the model-based formulation of the optimal DER dispatch problem, and motivate the need for a measurement-based approach. Section III outlines the estimation of the measurement-based sensitivity model. Section IV formulates the optimal DER dispatch problem with the estimated sensitivity model and presents the alternating direction method of multipliers (ADMM) solution approach. In Section V, we offer numerical case studies to demonstrate the effectiveness of the proposed measurement-based optimal DER dispatch framework. Finally, we provide concluding remarks and directions for future research in Section VI.

II. Preliminaries

In this section, we establish the system model and formulate the standard model-based optimal DER dispatch problem. We also motivate the need for a measurement-based approach.

A. Network and Power-flow Models

Consider a distribution system with N buses collected in the set $\mathcal{N} = \{1, \ldots, N\}$. Suppose pertinent system variables are sampled at time $t = k\Delta t$, $k = 0, 1, \ldots$, where Δt is the sampling interval. Let $V_{i,[k]}$ and $\theta_{i,[k]}$ denote, respectively, the voltage magnitude and phase-angle at bus i and discrete time step k. Also let $P_{i,[k]}$ and $Q_{i,[k]}$ denote, respectively, the net active- and reactive-power injections at bus i and time step k. Furthermore, collect voltage phase-angles and magnitudes at time step k in vector $x_{[k]} = [\theta_{1,[k]}, \ldots, \theta_{N,[k]}, V_{1,[k]}, \ldots, V_{N,[k]}]^{\mathrm{T}}$. Also collect net active- and reactive-power injections in vector $y_{[k]} = [P_{1,[k]}, \ldots, P_{N,[k]}, Q_{1,[k]}, \ldots, Q_{N,[k]}]^{\mathrm{T}}$. Then, power-flow equations at time step k can be compactly expressed as

$$y_{[k]} = g(x_{[k]}), \tag{1}$$

where $g : \mathbb{R}^{2N} \to \mathbb{R}^{2N}$. In (1), the dependence on network parameters (such as circuit breaker status and line impedances) is implicitly considered in the function $g(\cdot)$.

B. Optimal DER Dispatch Problem

We introduce an optimization problem to solve for DER setpoints that minimize a desired cost function (e.g., cost of DER generation, deviations from references, etc.) subject to

the nonlinear power balance (1) and other operational constraints.[1] To this end, let $P^{\text{gen}}_{i,[k]}$ and $Q^{\text{gen}}_{i,[k]}$ denote, respectively, the controllable components of active- and reactive-power injections at bus i and time step k; and collect these in vector $y^{\text{gen}}_{[k]} = [P^{\text{gen}}_{1,[k]}, \ldots, P^{\text{gen}}_{N,[k]}, Q^{\text{gen}}_{1,[k]}, \ldots, Q^{\text{gen}}_{N,[k]}]^{\text{T}}$. Similarly, collect the uncontrollable active- and reactive-power loads at all buses into vector $y^{\text{load}}_{[k]} \in \mathbb{R}^{2N}$, so that $y_{[k]} = y^{\text{gen}}_{[k]} - y^{\text{load}}_{[k]}$. The optimal DER dispatch problem can be formulated as

$$\underset{x_{[k]},\, y_{[k]},\, y^{\text{gen}}_{[k]}}{\text{minimize}} \quad f(x_{[k]}, y_{[k]}, y^{\text{gen}}_{[k]}), \tag{2a}$$

$$\text{subject to} \quad y_{[k]} = g(x_{[k]}) = y^{\text{gen}}_{[k]} - y^{\text{load}}_{[k]}, \tag{2b}$$

$$x_{\min} \le x_{[k]} \le x_{\max}, \tag{2c}$$

$$y^{\text{gen}}_{[k]} \in \mathcal{Y}^{\text{gen}}, \tag{2d}$$

where $f : \mathbb{R}^{2N} \times \mathbb{R}^{2N} \times \mathbb{R}^{2N} \to \mathbb{R}$ is the objective function to be minimized; $x_{\min}$ and $x_{\max}$ denote, respectively, minimum and maximum limits of voltage phase-angles and magnitudes; and $\mathcal{Y}^{\text{gen}}$ represents the (typically convex) space of allowable DER active- and reactive-power outputs [2]. In addition to minimum and maximum active- and reactive-power limits, typically DER outputs are constrained by the inverter apparent-power rating (more details are provided in [3]). The optimization problem in (2) is, in general, nonconvex and NP-hard (see, e.g., [28]).

C. Problem Statement

Repeatedly solving the optimization problem in (2) may pose significant computational hurdles for the utility operator in real time, especially with rapidly varying operating point. Furthermore, accurate solutions of (2) rely on an offline system model that represents the up-to-date network topology, parameters, and operating point, which may not be available due to insufficient telemetry from, e.g., all circuit breakers and load variations. Thus, aimed at practical field deployment, we use online measurements of nodal voltages and injections obtained at a subset of buses to estimate linear sensitivities and construct a linear voltage-to-power sensitivity model. We then incorporate the estimated linear sensitivity model as a proxy for the nonlinear power-balance constraint in a modified optimal DER dispatch problem based on (2). The proposed method accomplishes the objectives of (i) eliminating the reliance on an accurate offline model, (ii) removing requirement of a fully observable distribution system, and (iii) reducing the computational burden in solving the optimal DER setpoints.

III. Estimation of Sensitivity Model

In this section, we estimate the linear sensitivity model relating measured bus voltages and power injections via the RWPLS method without relying on an offline system model.

[1] In the remainder of the paper, quantities associated with power generation are marked by superscript "gen", and those associated with demand by superscript "load". Furthermore, measured or estimated quantities are marked by $\widehat{\cdot}$, and decision variables associated with measured buses by $\bar{\cdot}$.

A. Problem Formulation

Let $\mathcal{E} \subseteq \mathcal{N}$ represent the set of E buses equipped with D-PMUs, including the substation bus (set as bus 1 without loss of generality), where measurements of voltage phasors and power injections are collected. Assume that the substation-bus voltage is fixed and known, and let $\mathcal{E}^- = \mathcal{E} \setminus \{1\}$. Also denote by $\mathcal{D}$ the set of D buses that are connected to DERs, whose setpoints can be updated with each optimal dispatch solution. We assume that $\mathcal{D} \subseteq \mathcal{E}^-$, i.e., measurements are available at all buses with controllable DERs. Denote the measured voltage phase-angle and magnitude at bus $i \in \mathcal{E}^-$ and time step k as $\widehat{\theta}_{i,[k]}$ and $\widehat{V}_{i,[k]}$, respectively. Similarly, let $\widehat{P}_{i,[k]}$ and $\widehat{Q}_{i,[k]}$ denote the measured active- and reactive-power injections at bus $i \in \mathcal{E}$ and time step k. Accordingly, collect these quantities in vectors $\widehat{x}_{[k]} = [\{\widehat{\theta}_{i,[k]}\}_{i\in\mathcal{E}^-}, \{\widehat{V}_{i,[k]}\}_{i\in\mathcal{E}^-}]^{\text{T}}$ and $\widehat{y}_{[k]} = [\{\widehat{P}_{i,[k]}\}_{i\in\mathcal{E}}, \{\widehat{Q}_{i,[k]}\}_{i\in\mathcal{E}}]^{\text{T}}$. We hypothesize that the active- and reactive-power injections are linearly related to bus-voltage phase-angles and magnitudes, as follows:

$$\widehat{y}_{[k]} = J_{[k]}\widehat{x}_{[k]} + c_{[k]}, \tag{3}$$

where $J_{[k]}$ and $c_{[k]}$ form the sensitivity model relating measured voltages to power injections at the same buses. Then, there exists $H_{[k]} \in \mathbb{R}^{(2E-1)\times 2E}$ that satisfies the relationship:

$$\widehat{y}^{\text{T}}_{[k]} = \begin{bmatrix} \widehat{x}^{\text{T}}_{[k]} & 1 \end{bmatrix} H_{[k]}, \tag{4}$$

which is equivalent to (3) with $H_{[k]} = [J_{[k]}, c_{[k]}]^{\text{T}}$. In order to eliminate the reliance on a known network model, we propose to estimate the entries of $H_{[k]}$ using only online measurements obtained from buses in $\mathcal{E}$. To this end, suppose that M samples of bus-voltage angles and magnitudes, $\widehat{x}_{[k-M+1]}, \ldots, \widehat{x}_{[k]}$, and active- and reactive-power injections, $\widehat{y}_{[k-M+1]}, \ldots, \widehat{y}_{[k]}$, are available. Further suppose that the operating point remains approximately constant over the M measurement samples (we will remove this assumption later). Then, with $M > 2E$, we stack up M instances of (4) to yield the following over-determined system:

$$Y_{[k]} = X_{[k]}H_{[k]}, \tag{5}$$

where $X_{[k]} \in \mathbb{R}^{M\times(2E-1)}$ and $Y_{[k]} \in \mathbb{R}^{M\times 2E}$ are given by

$$X_{[k]} = \begin{bmatrix} \widehat{x}^{\text{T}}_{[k-M+1]} & 1 \\ \vdots & \vdots \\ \widehat{x}^{\text{T}}_{[k]} & 1 \end{bmatrix}, \quad Y_{[k]} = \begin{bmatrix} \widehat{y}^{\text{T}}_{[k-M+1]} \\ \vdots \\ \widehat{y}^{\text{T}}_{[k]} \end{bmatrix}. \tag{6}$$

Since (5) is over-determined, we can obtain the ordinary least-squares (OLS) estimate for $H_{[k]}$ as

$$\widehat{H}_{[k]} \approx (X^{\text{T}}_{[k]}X_{[k]})^{-1}X^{\text{T}}_{[k]}Y_{[k]}. \tag{7}$$

However, in practice, OLS estimation is challenged by the observation that voltage phase-angles and magnitudes at different buses may be highly correlated because they evolve similarly with variations in operating point [29], which results in an ill-conditioned regressor matrix $X^{\text{T}}_{[k]}X_{[k]}$ in (7). Furthermore, in order to capture changing operating conditions, it is desirable to update $\widehat{H}_{[k]}$ recursively while reducing computational burden. Also advantageous is to place greater emphasis on more

recent measurements than earlier ones that may become out of date over time. In light of these circumstances, we propose to use the RWPLS algorithm to compute $\widehat{H}_{[k]}$, as it offers several benefits over OLS estimation.

B. RWPLS-based Estimation

The potentially high collinearity in $X_{[k]}$ makes matrix inversion in (7) numerically challenging. A suitable solution approach in such a setting is the partial least-squares (PLS) method. The central idea in PLS is to project so-called *latent features* or key components in $X_{[k]}$ and $Y_{[k]}$ onto lower-dimensional latent matrices, which best model the relationship in (5). Then the least-squares regression is performed on the latent matrices. Particularly, given matrices constructed from online measurements $X_{[k]}$ and $Y_{[k]}$, the PLS algorithm returns

$$\{X_{[k]}, Y_{[k]}\} \xrightarrow{\text{PLS}} \{\Gamma_{[k]}, G_{[k]}, L_{[k]}\}, \tag{8}$$

where $G_{[k]}$ and $L_{[k]}$ are lower-dimensional loading matrices corresponding to $X_{[k]}$ and $Y_{[k]}$, respectively, and $\Gamma_{[k]}$ is a diagonal matrix with regression coefficients from the PLS decomposition. Then, the PLS estimate is given by

$$\widehat{H}_{[k]} = (G_{[k]}G_{[k]}^{\mathrm{T}})^{-1}G_{[k]}\Gamma_{[k]}L_{[k]}^{\mathrm{T}}. \tag{9}$$

The PLS method is summarized in Appendix A, and more details can be found in [30].

Now, suppose that at time step $k+1$, a new set of measurements, $\widehat{x}_{[k+1]}$ and $\widehat{y}_{[k+1]}$, becomes available, so that

$$X_{[k+1]} = \begin{bmatrix} X_{[k]} & \\ \widehat{x}_{[k+1]}^{\mathrm{T}} & 1 \end{bmatrix}, \quad Y_{[k+1]} = \begin{bmatrix} Y_{[k]} \\ \widehat{y}_{[k+1]}^{\mathrm{T}} \end{bmatrix}. \tag{10}$$

Then, following (8), the PLS method yields

$$\{X_{[k+1]}, Y_{[k+1]}\} \xrightarrow{\text{PLS}} \{\Gamma_{[k+1]}, G_{[k+1]}, L_{[k+1]}\}. \tag{11}$$

In other words, the PLS method solves the full regression problem by decomposing $X_{[k+1]}$ and $Y_{[k+1]}$ at the next time step $k+1$, but these repeated decompositions may be computationally burdensome in online implementation. A less computationally expensive, and indeed equivalent, alternative is to recursively update the estimated sensitivities by performing the PLS algorithm in (11) with (see, e.g., [30, Th. 1])

$$X_{[k+1]} = \begin{bmatrix} G_{[k]}^{\mathrm{T}} & \\ \widehat{x}_{[k+1]}^{\mathrm{T}} & 1 \end{bmatrix}, \quad Y_{[k+1]} = \begin{bmatrix} \Gamma_{[k]}L_{[k]}^{\mathrm{T}} \\ \widehat{y}_{[k+1]}^{\mathrm{T}} \end{bmatrix}, \tag{12}$$

leading to a lower-dimensional PLS decomposition problem. Furthermore, we can embed weight factors that prioritize more recent measurements over earlier ones. Particularly, the RWPLS method updates $\widehat{H}_{[k]}$ with the so-called *forgetting factor* $\sigma \in (0, 1]$ by making use of the procedure represented by (11), except with [30]

$$X_{[k+1]} = \begin{bmatrix} \sigma G_{[k]}^{\mathrm{T}} & \\ \widehat{x}_{[k+1]}^{\mathrm{T}} & 1 \end{bmatrix}, \quad Y_{[k+1]} = \begin{bmatrix} \sigma\Gamma_{[k]}L_{[k]}^{\mathrm{T}} \\ \widehat{y}_{[k+1]}^{\mathrm{T}} \end{bmatrix}. \tag{13}$$

In the above, if $\sigma < 1$, then earlier measurements would not contribute as much to the final estimate as more recent ones, i.e., weights of earlier measurements decrease exponentially as more data is acquired. This is especially useful for the case where the system experiences a change in operating point during the time window in which measurements are obtained. For online implementation, the initial estimate of the sensitivity model $\widehat{H}_{[k]}$ can be obtained using the standard PLS estimation (8)–(9) once a sufficient number of samples has been acquired. Then at each subsequent time step when a new set of measurements becomes available, the estimated model can be updated via (11) in conjunction with (13).

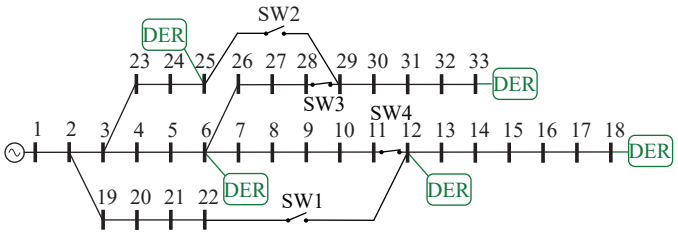

Fig. 1. IEEE 33-bus test system with DERs at buses $6, 12, 18, 25$, and 33; measurements are collected at bus 1 and all DER buses. Switches SW1 and SW2 are normally open, and switches SW3 and SW4 are normally closed.

Example 1 (Comparing OLS and PLS)**.** We present the numerical advantages of the PLS algorithm over OLS estimation via an example involving the IEEE 33-bus test system (see, e.g., [31]). The single-line diagram of the test system is shown in Fig. 1. We collect 25 sets of measurements of bus-voltage phase-angles and magnitudes as well as active- and reactive-power injections from D-PMUs installed at buses in the set $\mathcal{E} = \{1, 6, 12, 18, 25, 33\}$. Suppose that the active- and reactive-power components of loads at buses in $\mathcal{E}^- = \mathcal{E} \setminus \{1\}$ vary randomly around their nominal values as Gaussian distributed random variables with zero mean and 0.1% standard deviation relative to the respective nominal load values. We compare condition numbers of matrices that need to be inverted to obtain OLS and PLS estimates in (7) and (9), respectively. In OLS, the condition number of matrix $X_{[k]}^{\mathrm{T}}X_{[k]}$ is 1.2245×10^{15}, indicating that it is nearly singular. In contrast, the condition number of matrix $G_{[k]}G_{[k]}^{\mathrm{T}}$ is 6.5973, which leads to a numerically meaningful inverse and consequently an accurate linear sensitivity model relating measured voltages and injections. ■

IV. DER Dispatch Problem with Estimated Model

Instead of relying on an accurate offline model to solve the problem in (2), we leverage online measurements to estimate linear sensitivities and construct the sensitivity-based power-balance model in (3). In this section, we formulate an optimal DER dispatch problem that incorporates the estimated linear sensitivity model as a constraint and outline a tractable solution approach using the ADMM.

A. Problem Formulation

Let $\overline{x}_{[k+1]} = [\{\theta_{i,[k+1]}\}_{i\in\mathcal{E}^-}, \{V_{i,[k+1]}\}_{i\in\mathcal{E}^-}]^{\mathrm{T}}$ comprise nodal voltage phase-angles and magnitudes at buses equipped with D-PMUs and time step $k+1$. Note that the substation voltage is assumed to be fixed to its known reference value, so it is not included as a variable. In our problem, we determine optimal DER active- and reactive-power outputs

$\overline{y}^{\text{gen}}_{[k+1]} = [\{P^{\text{gen}}_{i,[k+1]}\}_{i\in\mathcal{D}}, \{Q^{\text{gen}}_{i,[k+1]}\}_{i\in\mathcal{D}}]^{\mathrm{T}}$ and, in turn, net injections $\overline{y}_{[k+1]} = [\{P_{i,[k+1]}\}_{i\in\mathcal{E}}, \{Q_{i,[k+1]}\}_{i\in\mathcal{E}}]^{\mathrm{T}}$ while satisfying operational constraints on $\overline{x}_{[k+1]}$, $\overline{y}_{[k+1]}$, and $\overline{y}^{\text{gen}}_{[k+1]}$. Note that $\overline{y}_{[k+1]}$ includes the substation injections so that we can achieve feeder-level active- and reactive-power regulation. With the above notation in place, we propose to solve the following optimization problem:

$$\underset{\overline{x}_{[k+1]},\overline{y}_{[k+1]},\overline{y}^{\text{gen}}_{[k+1]}}{\text{minimize}} \quad f(\overline{x}_{[k+1]}, \overline{y}_{[k+1]}, \overline{y}^{\text{gen}}_{[k+1]}), \tag{14a}$$

$$\text{subject to} \quad \overline{y}_{[k+1]} = J_{[k]}\overline{x}_{[k+1]} + c_{[k]}, \tag{14b}$$

$$\overline{y}_{[k+1]} = \overline{y}_{[k]} + C(\overline{y}^{\text{gen}}_{[k+1]} - \overline{y}^{\text{gen}}_{[k]}), \tag{14c}$$

$$\overline{x}_{\min} \le \overline{x}_{[k+1]} \le \overline{x}_{\max}, \tag{14d}$$

$$\overline{y}^{\text{gen}}_{[k+1]} \in \overline{\mathcal{Y}}^{\text{gen}}, \tag{14e}$$

where $\overline{x}_{\min}$ and $\overline{x}_{\max}$ represent, respectively, the minimum and maximum limits of voltage phase-angles and magnitudes at buses that are measured, and $\overline{\mathcal{Y}}^{\text{gen}}$ represents the allowable space of DER outputs. Under typical DER control schemes (including, e.g., active-power control, reactive-power control, and joint active- and reactive-power control), $\overline{\mathcal{Y}}^{\text{gen}}$ is convex [3]. Furthermore, in (14c), $C \in \mathbb{R}^{2E\times 2D}$ is the matrix that maps the DER bus indices to buses from which measurements are obtained. Particularly, the entry in the ith row and jth column of C is 1 if the jth element of $\overline{y}^{\text{gen}}_{[k+1]}$ is measured as the ith element of $\overline{y}_{[k+1]}$, and it is 0 otherwise. The constraint in (14c) results by recognizing that, at time steps k and $k+1$, respectively,

$$\overline{y}_{[k]} = C\overline{y}^{\text{gen}}_{[k]} - \overline{y}^{\text{load}}_{[k]}, \tag{15}$$

$$\overline{y}_{[k+1]} = C\overline{y}^{\text{gen}}_{[k+1]} - \overline{y}^{\text{load}}_{[k+1]}. \tag{16}$$

Assuming that the loads at the measured buses do not change significantly between time steps k and $k+1$, (16) can be expressed as

$$\overline{y}_{[k+1]} = C\overline{y}^{\text{gen}}_{[k+1]} - \overline{y}^{\text{load}}_{[k]}. \tag{17}$$

Suitably rearranging (15) and substituting the resultant into the above, we get the constraint in (14c). The entries of $J_{[k]}$ and $c_{[k]}$ may be computed from a model if one is at hand, or they can be estimated from online measurements, as discussed in Section III. In either case, the underlying assumption is that $J_{[k]}$ and $c_{[k]}$ computed or estimated at time step k model the relationship between $\overline{y}_{[k+1]}$ and $\overline{x}_{[k+1]}$ at time step $k+1$ with sufficient accuracy.

In (14), we utilize a quadratic cost function that comprises a weighted combination of (i) deviations of voltage phase-angles and magnitudes from their reference values, (ii) deviations of nodal active- and reactive-power injections from their setpoints, and (iii) cost of DER active- and reactive-power outputs. Thus, the cost function in (14) can be expressed as

$$\begin{aligned} f(\overline{x}_{[k+1]}, \overline{y}_{[k+1]}, \overline{y}^{\text{gen}}_{[k+1]}) = {} & (\overline{x}_{[k+1]} - \overline{x}^{\circ})^{\mathrm{T}}\Psi(\overline{x}_{[k+1]} - \overline{x}^{\circ}) \\ & + (\overline{y}_{[k+1]} - \overline{y}^{\circ})^{\mathrm{T}}\Phi(\overline{y}_{[k+1]} - \overline{y}^{\circ}) \\ & + (\overline{y}^{\text{gen}}_{[k+1]})^{\mathrm{T}}\Upsilon\overline{y}^{\text{gen}}_{[k+1]}, \end{aligned} \tag{18}$$

where $\overline{x}^{\circ}$ and $\overline{y}^{\circ}$, respectively, denote the desired voltage setpoints for DER buses and desired setpoints for power injections at measured buses. In (18), $\Psi = \text{diag}(\psi_1, \ldots, \psi_{2E-2})$, $\Phi = \text{diag}(\varphi_1, \ldots, \varphi_{2E})$, and $\Upsilon = \text{diag}(\upsilon_1, \ldots, \upsilon_{2D})$ are diagonal matrices with non-negative entries, i.e., $\psi_i, \varphi_i, \upsilon_i \ge 0$. The cost function in (18) is general in the sense that weight matrices Ψ, Φ, and Υ, respectively, enforce minimization in the cost of voltage-phasor deviations, power-injection deviations, and DER outputs.

With positive semidefinite weight matrices, (14) is a convex quadratic optimization problem that can be solved in polynomial time [32]. Particularly, by collecting decision variables in $\chi_{[k+1]} = [\overline{x}^{\mathrm{T}}_{[k+1]}, \overline{y}^{\mathrm{T}}_{[k+1]}, (\overline{y}^{\text{gen}}_{[k+1]})^{\mathrm{T}}]^{\mathrm{T}} \in \mathbb{R}^{4E+2D-2}$, the problem in (14) can be rewritten in the standard form of a convex quadratic program as follows:

$$\underset{\chi_{[k+1]}}{\text{minimize}} \quad \frac{1}{2}\chi^{\mathrm{T}}_{[k+1]}\Pi\chi_{[k+1]} + \pi^{\mathrm{T}}\chi_{[k+1]} + \kappa, \tag{19a}$$

$$\text{subject to} \quad A_{[k]}\chi_{[k+1]} = b_{[k]}, \tag{19b}$$

$$\chi_{[k+1]} \in \mathcal{X}. \tag{19c}$$

Entries in and structures of Π, π, κ, $A_{[k]}$, $b_{[k]}$, and $\mathcal{X}$ are detailed in Appendix B. Subsequently, we remove the constant term κ from (19a) as it does not affect the solution of the optimization problem.

B. ADMM-based Solution Approach

The problem in (19) can be solved using ADMM, which is a tractable method as each subproblem in the ADMM admits a closed-form solution in our setting. Also, the ADMM converges in linear time in our problem setting [33]. To begin, define an auxiliary variable $\omega_{[k+1]}$ so that the equality constraint and the bound constraint in (19b) and (19c), respectively, are associated with different variables. Then the problem in (19) can be reformulated as follows:

$$\underset{\chi_{[k+1]},\,\omega_{[k+1]}}{\text{minimize}} \quad \frac{1}{2}\chi^{\mathrm{T}}_{[k+1]}\Pi\chi_{[k+1]} + \pi^{\mathrm{T}}\chi_{[k+1]}, \tag{20a}$$

$$\text{subject to} \quad A_{[k]}\chi_{[k+1]} = b_{[k]}, \tag{20b}$$

$$\omega_{[k+1]} \in \mathcal{X}, \tag{20c}$$

$$\chi_{[k+1]} = \omega_{[k+1]}. \tag{20d}$$

In (20), the equality and inequality constraints involve different variables, coupled by the constraint in (20d). The ADMM alternates between solving an equality-constrained quadratic program with decision variable $\chi_{[k+1]}$ and a projection onto bound constraints with decision variable $\omega_{[k+1]}$. The augmented Lagrangian associated with (20) is given by [32]

$$\begin{aligned} \mathcal{L}_{\rho}(\chi_{[k+1]}, \omega_{[k+1]}, \mu_{[k+1]}) = {} & \frac{1}{2}\chi^{\mathrm{T}}_{[k+1]}\Pi\chi_{[k+1]} + \pi^{\mathrm{T}}\chi_{[k+1]} \\ & + \frac{\rho_{[k]}}{2}\left\|\chi_{[k+1]} - \omega_{[k+1]} - \mu_{[k+1]}\right\|_2^2 \\ & - \frac{\rho_{[k]}}{2}\left\|\mu_{[k+1]}\right\|_2^2, \end{aligned} \tag{21}$$

where $\rho_{[k]}$ is a positive scalar and $\mu_{[k+1]}$ is the scaled dual variable for the coupling constraint in (20d). The value of the ADMM parameter $\rho_{[k]}$ for optimal convergence is given by

$$\rho_{[k]} = \sqrt{\lambda_{\min}(Z^{\mathrm{T}}_{[k]}\Pi Z_{[k]})\lambda_{\max}(Z^{\mathrm{T}}_{[k]}\Pi Z_{[k]})}, \tag{22}$$

where $\lambda_{\min}(\cdot)$ and $\lambda_{\max}(\cdot)$, respectively, represent the minimum and the maximum eigenvalues of their arguments,

and $Z_{[k]}$ an orthonormal basis for the null space of $A_{[k]}$ [32]. Interested readers are referred to [32] for further background on ADMM and its convergence properties. Below, we briefly summarize the iterative solution procedure used in numerical case studies presented in Section V.

The ADMM uses a sequence of iterations indexed by ℓ to search for the minimizer of (20), as follows:

$$\chi_{[k+1]}^{\ell+1} = \arg \underset{\chi_{[k+1]}}{\text{minimize}} \quad \mathcal{L}_\rho(\chi_{[k+1]}, \omega_{[k+1]}^{\ell}, \mu_{[k+1]}^{\ell}), \\ \text{subject to} \quad A_{[k]}\chi_{[k+1]} = b_{[k]}, \tag{23}$$

$$\omega_{[k+1]}^{\ell+1} = \arg \underset{\omega_{[k+1]}}{\text{minimize}} \quad \mathcal{L}_\rho(\chi_{[k+1]}^{\ell+1}, \omega_{[k+1]}, \mu_{[k+1]}^{\ell}), \\ \text{subject to} \quad \omega_{[k+1]} \in \mathcal{X}, \tag{24}$$

$$\mu_{[k+1]}^{\ell+1} = \mu_{[k+1]}^{\ell} + \omega_{[k+1]}^{\ell+1} - \chi_{[k+1]}^{\ell+1}, \tag{25}$$

until $||\chi_{[k+1]}^{\ell} - \omega_{[k+1]}^{\ell}||_2 < \epsilon$ and $||\rho_{[k]}(\omega_{[k+1]}^{\ell} - \omega_{[k+1]}^{\ell-1})||_2 < \epsilon$, for some predefined tolerance $\epsilon > 0$, along with initial conditions $\chi_{[k+1]}^{0} = 0$, $\omega_{[k+1]}^{0} = 0$, and $\mu_{[k+1]}^{0} = 0$. The first step in each ADMM iteration is to update $\chi_{[k+1]}$ by solving (23), which has a closed-form solution (see, e.g., [32]). Next, with the updated $\chi_{[k+1]}^{\ell+1}$, $\omega_{[k+1]}^{\ell+1}$ is obtained by projecting $\chi_{[k+1]}^{\ell+1} - \mu_{[k+1]}^{\ell}$ onto the feasible set $\mathcal{X}$. Hence, the $\omega_{[k+1]}^{\ell+1}$-update in (24) equivalently recovers the following:

$$\omega_{[k+1]}^{\ell+1} = \arg \underset{\omega_{[k+1]} \in \mathcal{X}}{\text{minimize}} \ \frac{1}{2} \left\| \chi_{[k+1]}^{\ell+1} - \omega_{[k+1]} - \mu_{[k+1]}^{\ell} \right\|_2^2, \tag{26}$$

which also admits a closed-form solution for voltage bounds and typical constraints on DER outputs [3]. As a specific example, projections onto box constraints can be obtained as follows:

$$\omega_{[k+1]}^{\ell+1} = \min(\chi_{\max}, \max(\chi_{\min}, \chi_{[k+1]}^{\ell+1} - \mu_{[k+1]}^{\ell})), \tag{27}$$

where $\chi_{\min}$ and $\chi_{\max}$ comprise, respectively, the entry-wise lower and upper bounds of $\chi_{[k+1]}$. The update in (27) can be computed for each entry of $\omega_{[k+1]}^{\ell+1}$ independently. We refer interested readers to [3] for closed-form solutions to projections onto other typical allowable spaces of DER outputs. Finally, in each iteration, $\mu_{[k+1]}^{\ell+1}$ is obtained via (25) with updated values of $\chi_{[k+1]}^{\ell+1}$ and $\omega_{[k+1]}^{\ell+1}$. The ADMM iterations continue until the stopping criteria are satisfied with optimizers given by $\chi_{[k+1]}^{\star}$, $\omega_{[k+1]}^{\star}$, and $\mu_{[k+1]}^{\star}$, from which optimal DER dispatch $\overline{y}_{[k+1]}^{\text{gen}\star}$ (i.e., $P_{i,[k+1]}^{\text{gen}\star}$ and $Q_{i,[k+1]}^{\text{gen}\star}$, $i \in \mathcal{D}$) can be extracted.

V. Case Studies

In this section, we demonstrate the effectiveness of the measurement-based optimal DER dispatch framework proposed in Sections III–IV via numerical case studies involving the IEEE 33-bus test system introduced in Example 1 (see Fig. 1 for its one-line diagram), in which the power base is set to 10 MVA. Through the case studies, we show that the proposed measurement-based optimal DER dispatch (i) adapts to changes in topology and operating point, (ii) closely matches results obtained from model-based optimization approach with accurate system model, and (iii) outperforms model-based approach with outdated system model. We further evaluate the impact of DER dynamics, dispatch delays, and RWPLS parameters on the performance of the proposed method via simulations. In addition, we illustrate the flexibility of the proposed framework by considering typical constraints on DER outputs. Finally, we report execution times involved with the model estimation and optimal dispatch stages of the proposed framework.

A. Simulation Setup

Assume that DERs are connected to $D = 5$ buses in the set $\mathcal{D} = \{6, 12, 18, 25, 33\}$, as annotated in Fig. 1. Their active- and reactive-power outputs are, respectively, constrained within $P_i^{\text{gen}} \in [-0.25, 0.25]$ p.u. and $Q_i^{\text{gen}} \in [-0.25, 0.25]$ p.u. For all other buses $j \in \mathcal{N} \setminus \mathcal{D}$, $P_j^{\text{gen}} = Q_j^{\text{gen}} = 0$. Although our simulations (for now) focus on box constraints for the DER active- and reactive-power outputs, the problem formulation and the ADMM solution method outlined in Section IV can, in general, accommodate constraints delineated by typical DER operational limits (as we will demonstrate in Section V-E). Assume that voltage phasors and active- and reactive-power injections at $E = 6$ buses in $\mathcal{E} = \mathcal{D} \cup \{1\}$ are sampled at 1-second intervals. With each new set of measurements, the sensitivity model is updated via RWPLS by performing PLS with (13). Optimal dispatch is solved at 1-second intervals when DERs are active. In the proposed measurement-based method, the optimal dispatch is obtained via the ADMM solution to (20) immediately after an updated sensitivity model is estimated.

We dispatch DER active- and reactive-power setpoints to simultaneously (i) minimize voltage-magnitude deviations from reference levels (1 p.u. in our case studies), (ii) regulate the active-power injections at the substation bus 1 and at bus 33, and (iii) minimize cost of DER active- and reactive-power outputs. To realize the above objectives, we set the diagonal entries in weight matrix Ψ as $\psi_i = 0$ for $i = 1, \ldots, D$ (corresponding to voltage phase-angles) and $\psi_i = 10$ for $i = D+1, \ldots, 2D$ (corresponding to voltage magnitudes). Furthermore, we set appropriate entries in $\overline{x}^{\circ}$ to reference voltage magnitude 1 p.u., i.e., $\overline{x}^{\circ} = [0_D^{\text{T}}, 1_D^{\text{T}}]^{\text{T}}$, where 0_D and 1_D denote the length-D vectors of all 0s and 1s, respectively. Diagonal entries in weight matrix Υ corresponding to costs of DER outputs are set to various values between 0.04 and 0.1 to reflect potentially different costs of distinct DER technologies. Finally, to demonstrate the ability for the proposed method to regulate the net power injection at a measured bus, the first entry (corresponding to bus 1) in $\overline{y}^{\circ}$ is set to the substation active-power reference of 0.3 p.u. and the Eth entry (corresponding to bus 33) is set to the active-power reference of 0.1 p.u.; accordingly, in Φ, φ_1 and φ_E are set to 10 while $\varphi_i = 0$ for $i = 2, \ldots, E-1, E+1, \ldots 2E$. The parameter values for our simulations are chosen in a fairly arbitrary manner, and the proposed optimal DER dispatch method can easily accommodate a different cost function of the form in (18).

B. Adaptability to Topology and Operating-point Changes

Suppose that the system initially operates without DER contribution, and the DERs are activated at time $t_{\text{start}} = 5$ s (time step $k_{\text{start}} = 5$). Subsequently, at time $t_\Delta = 10$ s (time step $k_\Delta = 10$), the system topology is reconfigured by closing

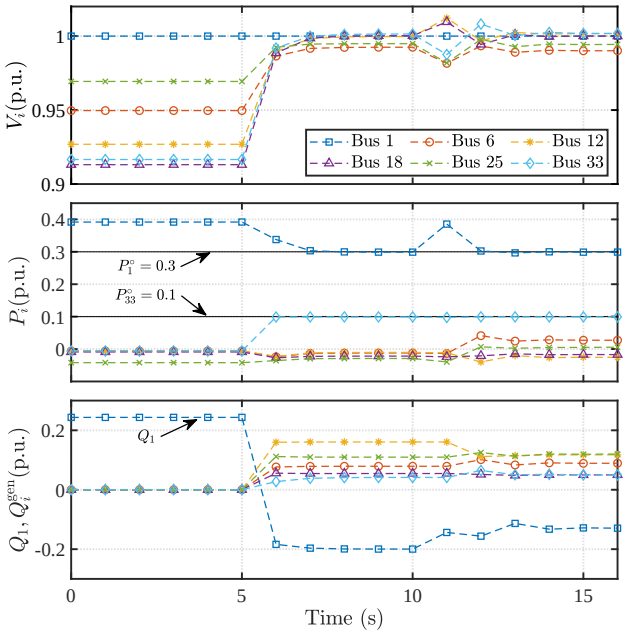

Fig. 2. Time-domain simulation via proposed measurement-based optimal DER dispatch. DERs are activated at time $t_{\text{start}} = 5\,\text{s}$ and the network topology and operating point are changed at time $t_\Delta = 10\,\text{s}$. Top pane: bus voltage magnitudes V_i at measured buses; Middle pane: bus active-power injections P_i at measured buses; Bottom pane: substation reactive-power injection Q_1 and DER reactive-power outputs Q_i^{gen} at controllable buses.

switches SW1 and SW2 and opening switches SW3 and SW4, and simultaneously, active- and reactive-power loads at all buses in the system grow by 25%. Simulations run until time $t_{\text{end}} = 16\,\text{s}$ (time step $k_{\text{end}} = 16$). The RWPLS forgetting factor is set to $\sigma = 0.6$.

1) Simulation Results: Time evolution of bus voltage magnitudes, as well as bus active-power injections and DER reactive-power outputs resulting from simulating the scenario described above with the proposed measurement-based DER dispatch method are plotted in Fig. 2. Indeed, once DERs are activated at time $t_{\text{start}} = 5\,\text{s}$, we observe that the proposed measurement-based dispatch effectively achieves the weighted objectives of minimizing voltage-magnitude deviations from 1 p.u., and regulating the active-power injections at the substation bus 1 and at bus 33 to 0.3 p.u. and 0.1 p.u., respectively. Upon activation of DERs, the substation reactive-power injection decreases sharply since DERs collectively provide voltage support by injecting reactive power, as shown in the bottom pane of Fig. 2. Also, after network-topology and operating-point changes at time $t_\Delta = 10\,\text{s}$, the proposed method updates the linear sensitivity model and adjusts the DER dispatch to achieve the same objectives. Our choices for Υ, Φ, and Ψ as described earlier optimize for a weighted objective. With different settings of Υ, Φ, and Ψ, other objectives, such as voltage control only, can be easily realized.

2) Comparisons to Model-based DER Dispatch: We benchmark the measurement-based optimal dispatch results presented above against the one obtained from the model-based problem in (2), which is solved with the MATPOWER Interior Point Solver (MIPS) [34]. We record the voltage profiles and bus active- and reactive-power injections, at $t_{\text{end}} = 16\,\text{s}$,

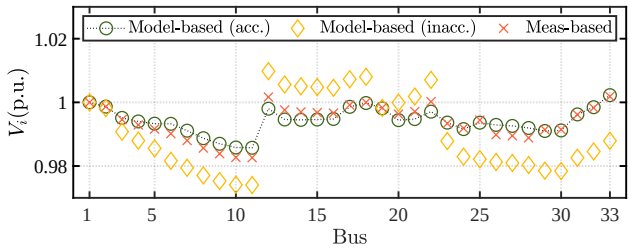

Fig. 3. Bus voltage magnitudes V_i at $t = 16\,\text{s}$ obtained via (i) model-based method with accurate system model, (ii) model-based method with inaccurate system model, and (iii) proposed measurement-based method. Voltage profile resulting from the proposed measurement-based method matches that from model-based benchmark with accurate system model, and it outperforms the model-based approach when the system model is not updated.

TABLE I
COMPARISON OF RELATIVE ERRORS IN COST FUNCTION, VOLTAGE MAGNITUDES, AND ACTIVE- AND REACTIVE-POWER DISPATCH AMONG (I) MODEL-BASED DER DISPATCH WITH ACCURATE SYSTEM MODEL, (II) MODEL-BASED DER DISPATCH WITH INACCURATE SYSTEM MODEL, AND (III) PROPOSED MEASUREMENT-BASED DER DISPATCH.

	Cost function (p.u.)	Cost function error (%)	Voltage-magnitude error (%)	Active-power error (%)	Reactive-power error (%)
Model-based (acc.)	0.0044	—	—	—	—
Model-based (inacc.)	0.0668	1872.75	0.94	15.47	12.63
Meas-based	0.0047	6.17	0.17	3.22	7.34

resulting from optimal DER dispatch setpoints obtained via (i) model-based approach assuming that the topology and operating-point changes are accurately captured in the model, (ii) model-based approach assuming that the model is not updated after the system changes at $t_\Delta = 10\,\text{s}$, and (iii) the proposed measurement-based approach. Figure 3 plots bus voltage magnitudes resulting from the three cases, and Table I summarizes errors in cases (ii) and (iii) as compared to the benchmark case (i). Results from the proposed method indeed match very closely to those from model-based optimal dispatch with accurate system model, with respect to the cost function value, voltage magnitudes, as well as resulting active- and reactive-power injections. Moreover, the measurement-based approach outperforms the model-based one when the system model is not updated to reflect the changes implemented at time $t_\Delta = 10\,\text{s}$. Although we consider topology and load changes in this case study, the proposed framework is flexible in that the optimal DER dispatch can easily adapt to other operating-point changes resulting from conventional distribution-level control mechanisms, including, e.g., switched capacitors and on-load tap changing transformers for voltage regulation.

C. Effect of RWPLS Forgetting Factor

The performance of the measurement-based DER dispatch method depends significantly on the value of the forgetting factor σ in the RWPLS estimation. To see this, we compare cost-function values obtained using (i) model-based dispatch vs. (ii) measurement-based dispatch by evaluating their root-mean-square-deviation (RMSD), given by

$$\text{RMSD} = \sqrt{\frac{1}{k_{\text{end}} - k_\Delta} \sum_{k=k_\Delta+1}^{k_{\text{end}}} (f_{[k]}^{\text{model}} - f_{[k]}^{\text{meas}})^2}, \quad (28)$$

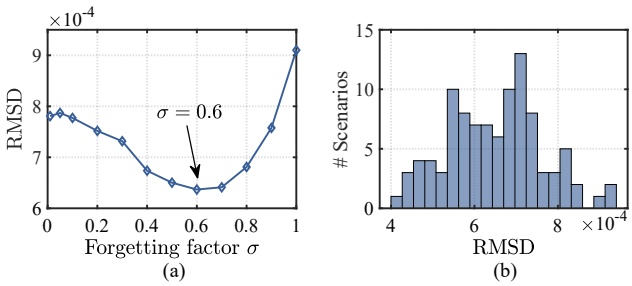

Fig. 4. Effect of forgetting factor in RWPLS algorithm on dispatch accuracy. (a) Mean cost-function RMSDs among model-based dispatch and measurement-based dispatch with different forgetting factors σ for 100 repeated simulations. (b) Histogram of RMSD values for the repeated simulations, with best parameter choice ($\sigma = 0.6$).

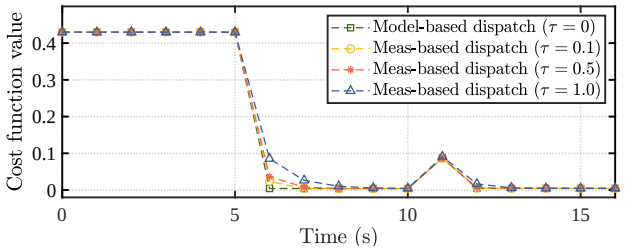

Fig. 5. Evaluation of cost function value over time for different DER time constants τ with the measurement-based DER dispatch method, compared to the model-based method with ideal DERs.

where $k_\Delta = 10$ is the time step when the network-topology and operating-point changes occur, and $k_{\text{end}} = 16$ is the last time step of the simulation. We set the forgetting factor ranging from 0.01 to 1, and for each, we conduct 100 repeated simulations set up as described in Sections V-A and V-B with random Gaussian-distributed load increases of $(25 \pm 1)\%$ at time step $t_\Delta = 10\,\text{s}$ and compute the average RMSD over all 100 simulations. The average RMSD values for different forgetting factors are plotted in Fig. 4a. We find that setting the forgetting factor $\sigma = 0.6$ yields the lowest errors. Furthermore, Fig. 4b shows a histogram representing the distribution of RMSD values for the 100 repeated simulations with forgetting factor $\sigma = 0.6$, with most scenarios centered around an RMSD value of 6×10^{-4}. Considering these observations, we set $\sigma = 0.6$ for simulations presented in Section V-B.

D. Effect of DER Dynamics and Delays

In practice, DER outputs do not change immediately after a new setpoint is dispatched. We adopt a first-order model for the DERs, similar to [1]. Simulations are performed with the setup described in Sections V-A and V-B along with DER time constants of $\tau = 0.1, 0.5, 1\,\text{s}$. The evaluated cost function at each time step are plotted in Fig. 5. We see that the proposed method is robust against slow-responding DERs, and the combined estimation/optimization routine converges to the optimal value achieved by the model-based benchmark.

Furthermore, we evaluate the robustness of the proposed method against delays between instants that measurements are acquired and DER setpoints are actuated. In practice, such delays may be attributed to communication, computation,

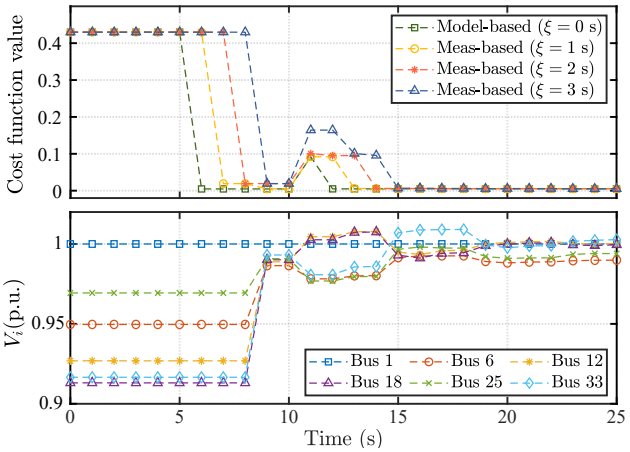

Fig. 6. Effect of delays between measurement acquisition and DER actuation. DERs are activated at time $t_{\text{start}} = 5\,\text{s}$ and the network topology and operating point are changed at time $t_\Delta = 10\,\text{s}$. Top pane: evaluation of cost function value over time for different DER dispatch delays ξ with the measurement-based DER dispatch method, compared to the model-based method without delay; Bottom pane: bus voltage magnitudes V_i at measured buses in case DER actuation is delayed by $\xi = 3\,\text{s}$.

and actuation. We adopt a similar simulation setup as in Sections V-A and V-B, except the DER dispatch is artificially delayed and simulations run until time $t_{\text{end}} = 25\,\text{s}$. We evaluate the cost function value at each time step and plot the resulting data points in the top pane of Fig. 6, where we use the model-based optimal DER dispatch without delay as a benchmark and compare it to the proposed measurement-based dispatch with delay of $\xi = 1, 2, 3\,\text{s}$. We observe that the combined estimation and optimization routine converges to the optimal value achieved by the model-based benchmark, albeit with a delay as expected. In the bottom pane of Fig. 6, we plot time evolution of bus-voltage magnitudes for $\xi = 3\,\text{s}$. We note that the significant network reconfiguration and network-wide load changes do not cause voltage constraint violations in the simulation. Moreover, the proposed method converges to the new optimal operating point within a reasonable amount of time even in the presence of delays.

E. Consideration of Typical DER Constraints

Some DER technologies may have different operational constraints than the independent active- and reactive-power limits considered in the case studies thus far. In this case study, we consider the DER dispatch resulting from scenarios in which each DER i has (i) independent active- and reactive-power limits, constrained within $P_i^{\text{gen}} \in [-0.1, 0.1]\,\text{p.u.}$ and $Q_i^{\text{gen}} \in [-0.1, 0.1]\,\text{p.u.}$, respectively, and (ii) joint active- and reactive-power limits, constrained by the apparent-power limit, where $\sqrt{(P_i^{\text{gen}})^2 + (Q_i^{\text{gen}})^2} \leq 0.1\,\text{p.u.}$ The projection step (26) in ADMM yields closed-form solutions under both of these DER output limits. Specifically, we utilize (27) to compute the projection onto box constraints, and we leverage a closed-form solution similar to the one in [3] for the projection onto the allowable region delineated by apparent-power limits. As shown in Fig. 7a, the DER outputs are indeed within the independent active- and reactive-power limits, whereas in

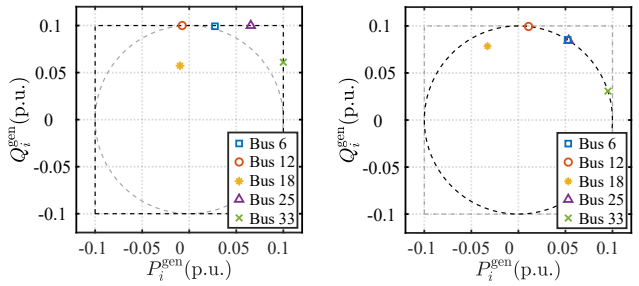

Fig. 7. DER active- and reactive-power outputs obtained via the measurement-based method when each DER is constrained by (a) independent active- and reactive-power limits, (b) its maximum apparent power.

TABLE II
COMPUTATION TIMES FOR (I) SENSITIVITY MODEL ESTIMATION (t_{est}), (II) OPTIMAL DER DISPATCH VIA ADMM (t_{ADMM}), AND (III) OPTIMAL DER DISPATCH VIA MATLAB'S STANDARD SOLVER `QUADPROG` (t_{IP})

# DERs	5	10	20	40	60	80	100
t_{est}(s)	0.0015	0.0033	0.0086	0.0389	0.2130	0.3643	0.5570
t_{ADMM}(s)	0.0177	0.0263	0.0904	0.2025	0.4016	0.5954	1.0548
t_{IP}(s)	0.0182	0.0252	0.0457	0.0609	0.1231	0.3711	1.2234

Fig. 7b, DER outputs are constrained by the apparent-power limit of 0.1 p.u. We note that the more constrained scenario of having apparent-power limits increases the resulting steady-state cost function value from 0.0052 to 0.0095. This simulation scenario illustrates that the proposed method using the ADMM can accommodate typical constraints on DER outputs.

F. Execution Times

To assess the computational burden and the scalability of the proposed measurement-based framework, we report execution times involving the 874-bus test system from [35], in which up to 100 DERs are installed at random locations. In Table II, we report the execution times required to (i) update the linear sensitivity model (t_{est}), and (ii) solve the convex quadratic DER dispatch problem using ADMM (t_{ADMM}), and (iii) solve the same problem using the interior-point solver from MATLAB `quadprog` (t_{IP}). All algorithms are run using MATLAB R2018b on a personal computer with Intel Core i5-8250U processor at 1.60 GHz, and 8 GB RAM. We find that the method can be executed in near real time for up to 100 DERs with the relatively limited computational resources available on a personal computer.

VI. Concluding Remarks

In this paper, we present a measurement-based framework to dispatch optimal DER active- and reactive-power outputs without relying on a system model. Optimal DER setpoints are obtained by embedding a recursively estimated sensitivity model as an equality constraint in a convex quadratic optimization problem, which is solved via ADMM. As demonstrated by numerical case studies, the main advantages of the proposed method are (i) combined minimization of bus voltage and injection deviations from prescribed references, as well as cost of DER outputs, (ii) accuracy of resulting DER setpoints without relying on a system model as compared to a model-based benchmark, (iii) adaptability to operating-point and network-topology changes, and (iv) modest computational burden. Compelling directions for future work include extension to unbalanced three-phase networks, distributed implementation, and consideration of DER and load uncertainty. Furthermore, incorporation of the estimated linear sensitivity model into other model-based optimal DER dispatch problems (e.g., [3], [19], [20]) is fertile grounds for future research.

Appendix

A. Deriving Partial Least-squares Estimate in (9)

The decompositions of $X_{[k]}$ and $Y_{[k]}$ are performed in a way to satisfy an outer model given by [30]

$$X_{[k]} = T_{[k]} G_{[k]}^{\mathrm{T}}, \tag{29}$$

$$Y_{[k]} = U_{[k]} L_{[k]}^{\mathrm{T}}, \tag{30}$$

where $T_{[k]} = [t_{[k],1}, \ldots, t_{[k],r}]$ (an orthonormal matrix) and $U_{[k]} = [u_{[k],1}, \ldots, u_{[k],r}]$ are latent matrices, each with $r \leq 2E-1$ score vectors $t_{[k],i}$ and $u_{[k],i}$, $i = 1, \ldots, r$, extracted from matrices $X_{[k]}$ and $Y_{[k]}$, $G_{[k]} = [g_{[k],1}, \ldots, g_{[k],r}]$ and $L_{[k]} = [l_{[k],1}, \ldots, l_{[k],r}]$ are corresponding loading matrices, with r loading vectors $g_{[k],i}$ and $l_{[k],i}$, $i = 1, \ldots, r$. Using the nonlinear iterative partial least squares (NIPALS) algorithm, $T_{[k]}$, $U_{[k]}$, $G_{[k]}$, and $L_{[k]}$ are populated in column-wise fashion [30].

The NIPALS algorithm maximizes the covariance between the score vectors $u_{[k],i}$ and $t_{[k],i}$, for all $i = 1, \ldots, r$, thereby forming the following inner model:

$$U_{[k]} = T_{[k]} \Gamma_{[k]}, \tag{31}$$

where $\Gamma_{[k]} = \mathrm{diag}(\gamma_{[k],1}, \ldots, \gamma_{[k],r})$, with

$$\gamma_{[k],i} = \frac{u_{[k],i}^{\mathrm{T}} t_{[k],i}}{t_{[k],i}^{\mathrm{T}} t_{[k],i}}. \tag{32}$$

The PLS regression is then performed on the over-determined inner model (31) instead of the original data set in $X_{[k]}$ and $Y_{[k]}$. Specifically, by substituting (31) into (30), we get

$$Y_{[k]} = T_{[k]} \Gamma_{[k]} L_{[k]}^{\mathrm{T}}. \tag{33}$$

Then, substitution of (29) and (33) into (7) while recognizing that $T_{[k]}$ is orthonormal yields (9), as desired. Interested readers may refer to [30] for background on the PLS method and details of the NIPALS algorithm.

B. Reformulating (14) as Standard Quadratic Program

In (19a), $\Pi \in \mathbb{R}^{(4E+2D-2)\times(4E+2D-2)}$, $\pi \in \mathbb{R}^{4E+2D-2}$, and $\kappa \in \mathbb{R}$ are obtained by suitable algebraic manipulations of (18); and they are given by

$$\Pi = 2 \begin{bmatrix} \Psi & 0 & 0 \\ 0 & \Phi & 0 \\ 0 & 0 & \Upsilon \end{bmatrix}, \quad \pi = -2 \begin{bmatrix} \Psi \overline{x}^{\circ} \\ \Phi \overline{y}^{\circ} \\ 0 \end{bmatrix}, \tag{34}$$

$$\kappa = (\overline{x}^{\circ})^{\mathrm{T}} \Psi \overline{x}^{\circ} + (\overline{y}^{\circ})^{\mathrm{T}} \Phi \overline{y}^{\circ}, \tag{35}$$

where 0s are matrices or vectors of all zeros with appropriate dimension. The linear constraints in (19b) is constructed by combining (14b) and (14c) with

$$A_{[k]} = \begin{bmatrix} -J_{[k]} & I_{2E} & 0 \\ 0 & I_{2E} & -C \end{bmatrix}, \; b_{[k]} = \begin{bmatrix} c_{[k]} \\ \overline{y}_{[k]} - C\overline{y}^{\text{gen}}_{[k]} \end{bmatrix}, \quad (36)$$

where I_{2E} denotes the $2E \times 2E$ identity matrix and 0s represent matrices of all zeros with appropriate dimension. Finally, $\mathcal{X}$ represents the composition of set constraints in (14d) and (14e).

REFERENCES

[1] E. Dall'Anese, S. S. Guggilam, A. Simonetto, Y. C. Chen, and S. V. Dhople, "Optimal regulation of virtual power plants," *IEEE Trans. Power Syst.*, vol. 33, no. 2, pp. 1868–1881, Mar. 2018.

[2] S. S. Guggilam, E. Dall'Anese, Y. C. Chen, S. V. Dhople, and G. B. Giannakis, "Scalable optimization methods for distribution networks with high PV integration," *IEEE Trans. Smart Grid*, vol. 7, no. 4, pp. 2061–2070, Jul. 2016.

[3] E. Dall'Anese and A. Simonetto, "Optimal power flow pursuit," *IEEE Trans. Smart Grid*, vol. 9, no. 2, pp. 942–952, Mar. 2018.

[4] A. von Meier, E. Stewart, A. McEachern, M. Andersen, and L. Mehrmanesh, "Precision micro-synchrophasors for distribution systems: a summary of applications," *IEEE Trans. Smart Grid*, vol. 8, no. 6, pp. 2926–2936, Nov. 2017.

[5] Y. Liu, N. Zhang, Y. Wang, J. Yang, and C. Kang, "Data-driven power flow linearization: a regression approach," *IEEE Trans. Smart Grid*, vol. 10, no. 3, pp. 2569–2580, May 2019.

[6] Y. Yuan, O. Ardakanian, S. Low, and C. Tomlin, "On the inverse power flow problem," *arXiv preprint arXiv:1610.06631v3*, Feb. 2020.

[7] J. Yu, Y. Weng, and R. Rajagopal, "PaToPa: A data-driven parameter and topology joint estimation framework in distribution grids," *IEEE Trans. Power Syst.*, vol. 33, no. 4, pp. 4335–4347, Jul. 2018.

[8] G. Cavraro and V. Kekatos, "Graph algorithms for topology identification using power grid probing," *IEEE Control Syst. Lett.*, vol. 2, no. 4, pp. 689–694, Oct. 2018.

[9] D. Deka, S. Backhaus, and M. Chertkov, "Structure learning in power distribution networks," *IEEE Trans. Control Netw. Syst.*, vol. 5, no. 3, pp. 1061–1074, Sep. 2018.

[10] O. Ardakanian, V. W. S. Wong, R. Dobbe, S. H. Low, A. von Meier, C. J. Tomlin, and Y. Yuan, "On identification of distribution grids," *IEEE Trans. Control Netw. Syst.*, vol. 6, no. 3, pp. 950–960, Sep. 2019.

[11] Y. C. Chen, A. D. Domínguez-García, and P. W. Sauer, "Measurement-based estimation of linear sensitivity distribution factors and applications," *IEEE Trans. Power Syst.*, vol. 29, no. 3, pp. 1372–1382, May 2014.

[12] Y. C. Chen, J. Wang, A. D. Domínguez-García, and P. W. Sauer, "Measurement-based estimation of the power flow Jacobian matrix," *IEEE Trans. Smart Grid*, vol. 7, no. 5, pp. 2507–2515, Sep. 2016.

[13] P. Li, H. Su, C. Wang, Z. Liu, and J. Wu, "PMU-based estimation of voltage-to-power sensitivity for distribution networks considering the sparsity of Jacobian matrix," *IEEE Access*, vol. 6, pp. 31 307–31 316, May 2018.

[14] C. Mugnier, K. Christakou, J. Jaton, M. De Vivo, M. Carpita, and M. Paolone, "Model-less/measurement-based computation of voltage sensitivities in unbalanced electrical distribution networks," in *Proc. of Power Syst. Comp. Conf.*, Jun. 2016.

[15] H. Xu, A. D. Domínguez-García, V. Veeravalli, and P. W. Sauer, "Data-driven voltage regulation in radial power distribution systems," *IEEE Trans. Power Syst.*, to be published.

[16] H. Su, P. Li, P. Li, X. Fu, L. Yu, and C. Wang, "Augmented sensitivity estimation based voltage control strategy of active distribution networks with PMU measurement," *IEEE Access*, vol. 7, pp. 44 987–44 997, Mar. 2019.

[17] H. Xu, A. D. Domínguez-García, and P. W. Sauer, "Data-driven coordination of distributed energy resources for active power provision," *IEEE Trans. Power Syst.*, vol. 34, no. 4, pp. 3047–3058, Jul. 2019.

[18] Y. Tang, K. Dvijotham, and S. Low, "Real-time optimal power flow," *IEEE Trans. Smart Grid*, vol. 8, no. 6, pp. 2963–2973, Nov. 2017.

[19] L. Ortmann, A. Hauswirth, I. Caduff, F. Dörfler, and S. Bolognani, "Experimental validation of feedback optimization in power distribution grids," *arXiv preprint arXiv:1910.03384*, Oct. 2019.

[20] M. Colombino, J. W. Simpson-Porco, and A. Bernstein, "Towards robustness guarantees for feedback-based optimization," *arXiv preprint arXiv:1905.07363*, May 2019.

[21] S. Bolognani, R. Carli, G. Cavraro, and S. Zampieri, "On the need for communication for voltage regulation of power distribution grids," *IEEE Trans. Control Netw. Syst.*, vol. 6, no. 3, pp. 1111–1123, Sep. 2019.

[22] G. Qu and N. Li, "Optimal distributed feedback voltage control under limited reactive power," *IEEE Trans. Power Syst.*, vol. 35, no. 1, pp. 315–331, Jan. 2020.

[23] C. Chang, M. Colombino, J. Cort, and E. Dall'Anese, "Saddle-flow dynamics for distributed feedback-based optimization," *IEEE Control Syst. Lett.*, vol. 3, no. 4, pp. 948–953, Oct. 2019.

[24] A. Bernstein and E. Dall'Anese, "Real-time feedback-based optimization of distribution grids: A unified approach," *IEEE Trans. Control Netw. Syst.*, vol. 6, no. 3, pp. 1197–1209, Sep. 2019.

[25] D. B. Arnold, M. D. Sankur, M. Negrete-Pincetic, and D. S. Callaway, "Model-free optimal coordination of distributed energy resources for provisioning transmission-level services," *IEEE Trans. Power Syst.*, vol. 33, no. 1, pp. 817–828, Jan. 2018.

[26] M. D. Sankur, R. Dobbe, A. von Meier, and D. B. Arnold, "Model-free optimal voltage phasor regulation in unbalanced distribution systems," *IEEE Trans. Smart Grid*, vol. 11, no. 1, pp. 884–894, Jan. 2020.

[27] S. Nowak, L. Wang, and Y. C. Chen, "Measurement-based optimal power flow with linear power-flow constraint for DER dispatch," in *Proc. of North American Power Symposium*, Oct. 2019.

[28] J. Lavaei and S. H. Low, "Zero duality gap in optimal power flow problem," *IEEE Trans. Power Syst.*, vol. 27, no. 1, pp. 92–107, Feb. 2012.

[29] J. Zhang, Z. Wang, X. Zheng, L. Guan, and C. Y. Chung, "Locally weighted ridge regression for power system online sensitivity identification considering data collinearity," *IEEE Trans. Power Syst.*, vol. 33, no. 2, pp. 1624–1634, Mar. 2018.

[30] S. J. Qin, "Recursive PLS algorithms for adaptive data modeling," *Computers & Chemical Engineering*, vol. 22, no. 4, pp. 503–514, Aug. 1998.

[31] M. E. Baran and F. F. Wu, "Network reconfiguration in distribution systems for loss reduction and load balancing," *IEEE Trans. Power Del.*, vol. 4, no. 2, pp. 1401–1407, Apr. 1989.

[32] A. U. Raghunathan and S. Di Cairano, "ADMM for convex quadratic programs: Q-linear convergence and infeasibility detection," *arXiv preprint arXiv:1411.7288*, Oct. 2014.

[33] E. Ghadimi, A. Teixeira, I. Shames, and M. Johansson, "Optimal parameter selection for the alternating direction method of multipliers (ADMM): Quadratic problems," *IEEE Trans. Autom. Control*, vol. 60, no. 3, pp. 644–658, Mar. 2015.

[34] R. D. Zimmerman, C. E. Murillo-Sánchez, and R. J. Thomas, "Matpower: steady-state operations, planning, and analysis tools for power systems research and education," *IEEE Trans. Power Syst.*, vol. 26, no. 1, pp. 12–19, Feb. 2011.

[35] H. Ahmadi, "874-node distribution test system," http://www.ece.ubc.ca/~hameda/download_files/node_874.m, online; Accessed: 2020-03-25.

Severin Nowak (S'16) received a B.Sc. degree in electrical engineering from the University of Applied Sciences in Fribourg, Switzerland in 2008.

He is currently a Ph.D. candidate at the School of Engineering, The University of British Columbia, Okanagan Campus in Kelowna, CA. His research interests include the modeling, simulation and control of modern power systems via measurement-based methods.

Yu Christine Chen (M'15) received the B.A.Sc. degree in engineering science from the University of Toronto, Toronto, ON, Canada, in 2009, and the M.S. and Ph.D. degrees in electrical engineering from the University of Illinois at Urbana-Champaign, Urbana, IL, USA, in 2011 and 2014, respectively. She is currently an Assistant Professor with the Department of Electrical and Computer Engineering, The University of British Columbia, Vancouver, BC, Canada, where she is affiliated with the Electric Power and Energy Systems Group. Her research interests include power system analysis, monitoring, and control.

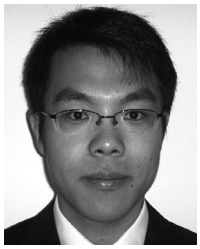

Liwei Wang (S'04 – M'10) received the M.S. degree in electrical engineering from Tianjin University, Tianjin, China, in 2004, and the Ph.D. degree in electrical and computer engineering from the University of British Columbia, Vancouver, BC, Canada, in 2010.

From February 2009 to July 2009, he was an Internship Researcher with the ABB Corporate Research Center, Baden-Dättwil, Switzerland. He was a Postdoctoral Research Fellow in the Department of Electrical and Computer Engineering, University of British Columbia, from February 2010 to July 2010. In August 2010, he joined the ABB Corporate Research Center, Västerås, Sweden, as a Scientist, and then as a Senior Scientist. Since July 2014, he has been an Assistant Professor in the Department of Electrical Engineering, University of British Columbia, Kelowna, BC, Canada. His research interests include power system analysis, operation, and simulation; electrical machines and drives; power electronics converter design, control, and topology; power semiconductor modeling and characterization; utility power electronics applications; HVDC and FACTS; renewable-energy sources; and distributed generation.